

# Monolithically Fabricated Microgripper With Integrated Force Sensor for Manipulating Microobjects and Biological Cells Aligned in an Ultrasonic Field

Felix Beyeler, *Student Member, IEEE*, Adrian Neild, Stefano Oberti, Dominik J. Bell, Yu Sun, *Member, IEEE*, Jürg Dual, and Bradley J. Nelson, *Member, IEEE*

**Abstract**—This paper reports an electrostatic microelectromechanical systems (MEMS) gripper with an integrated capacitive force sensor. The sensitivity is more than three orders of magnitude higher than other monolithically fabricated MEMS grippers with force feedback. This force sensing resolution provides feedback in the range of the forces that dominate the micromanipulation process. A MEMS ultrasonic device is described for aligning microobjects suspended in water using ultrasonic fields. The alignment of the particles is of a sufficient accuracy that the microgripper must only return to a fixed position in order to pick up particles less than 100  $\mu\text{m}$  in diameter. The concept is also demonstrated with HeLa cells, thus providing a useful tool in biological research and cell assays. [1744]

**Index Terms**—Capacitive force sensor, electrostatic microgripper, force feedback, handling biological cells, HeLa cancer cells, microelectromechanical systems (MEMS), micromanipulation, silicon-on-insulator (SOI) fabrication, ultrasonic positioning.

## I. INTRODUCTION

THE manipulation of objects on the microscale finds important applications in biological and biomedical research, as well as in the assembly of microelectromechanical systems (MEMS) and microelectronic devices. Micromanipulation of micrometer-sized parts requires the use of miniaturized grippers with end-effectors on the size-scale of the manipulated objects. Another requirement for such devices is that they allow for the controllable actuation of the gripper arms with a range and resolution of force and displacement matching the required size scale. MEMS technology allows for the fabrication of such devices that meet these requirements. Both suitable end-effectors and actuators can be fabricated with MEMS technology.

Several designs for microfabricated grippers with different types of actuators have been published in recent years. In 1991, a silicon electromechanical microgripper was presented [1]. The

manipulation of dried red-blood cells and various protozoa has been demonstrated in [2]. A polymer-based microgripper for single-cell manipulation has been reported in [3]. These grippers were designed without force feedback. Hybrid gripper designs have been demonstrated in [4] and [5] having integrated piezoresistive force sensors. A magnetically actuated gripper with piezoelectric force sensing has been reported in [6], and an optical method for force measurement is presented in [7]. These designs provide a reasonable sensitivity and resolution, but complicated and expensive assembly processes are required to build the grippers. Force measurement using optical methods is extremely difficult when working in liquids due to refraction and distortions of the light beam. In [8], an electrothermally actuated microgripper with integrated force sensor is presented. It is fabricated on the wafer level using a simple fabrication process. Unfortunately, the sensitivity is much lower compared to hybrid designs, making it impossible to measure the small forces dominating micromanipulation processes. For grippers to be useful in biomedical and biological applications, there are several requirements. Good control over their continuous movement is needed with force feedback in order to ensure that living objects such as cells or bacteria survive during manipulation. Another requirement results from the fact that a small device, such as a microgripper, can easily break during handling. Therefore, in order to minimize costs of a single device, the design must allow for its fabrication in batch. A monolithic design incorporating both actuator and force sensor is important for inexpensive and simple fabrication and implementation. Biocompatibility issues must also be considered. To be able to work with biological samples, such as living cells, it must be possible to immerse the gripper arms into liquids. Also, high temperatures in the gripper arms, as they are typical for thermally actuated grippers, should be avoided. With these requirements, a design based on an electrostatic actuator and a capacitive force sensor was identified as the most suitable alternative.

This paper presents a new design for such a gripper with electrostatic actuation and capacitive force sensing. The fabrication process is based on a process that was originally developed for multi-degree-of-freedom capacitive force sensors [9], [10]. First, gripper design and modelling is described. Then the fabrication process is explained. Furthermore, the fabricated gripper is illustrated along with the results from calibration of the actuator and force sensor.

Manuscript received January 9, 2006; revised August 7, 2006. This work was supported by KTI/CTI, Switzerland, under a Top Nano 21 Grant, Projects 6643.1 and 6989.1, and by the National Science Foundation, Switzerland, under Grant 205321-102213. Subject Editor C.-J. Kim.

F. Beyeler, D. J. Bell, and B. J. Nelson are with the Institute of Robotics and Intelligent Systems, Swiss Federal Institute of Technology, CH-8092 Zürich, Switzerland (e-mail: fbey@ethz.ch).

A. Neild, S. Oberti, and J. Dual are with the Center of Mechanics, Swiss Federal Institute of Technology, CH-8092 Zürich, Switzerland.

Y. Sun is with the Department of Mechanical and Industrial Engineering, University of Toronto, Toronto, ON, Canada.

Digital Object Identifier 10.1109/JMEMS.2006.885853

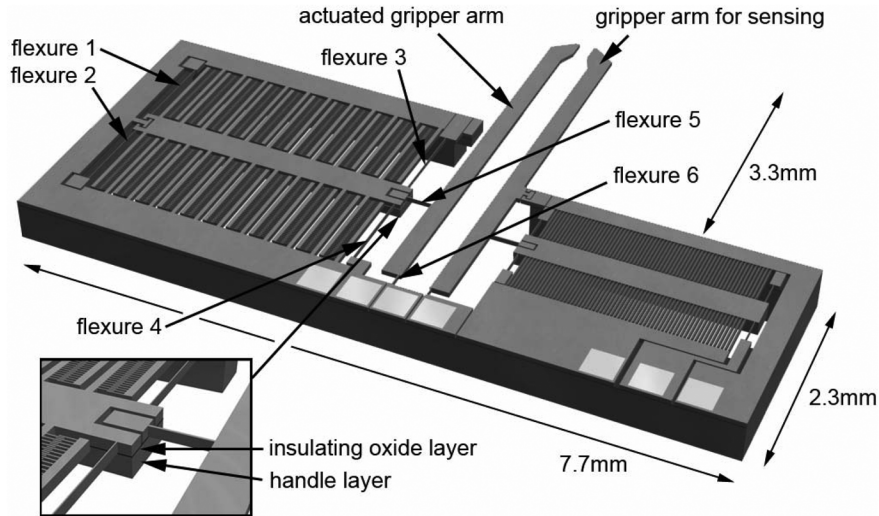


Fig. 1. Solid model of the microgripper with integrated force sensor.

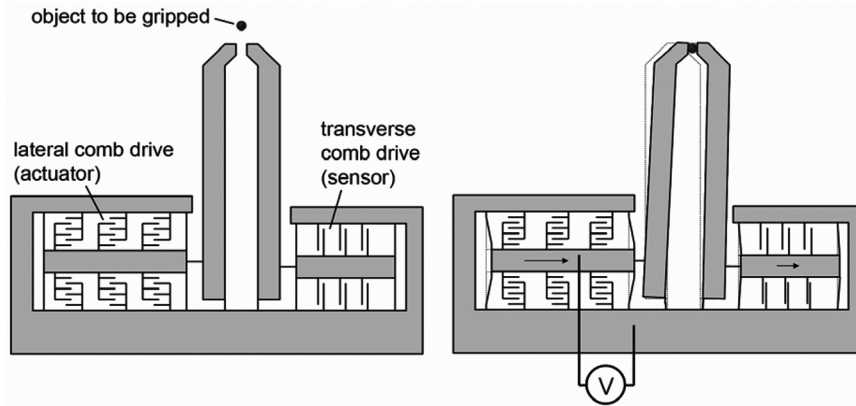


Fig. 2. Functional principle of the microgripper. By applying a voltage to the actuator, the gripping force can be measured as a deflection of the right gripper arm.

In addition, the gripper is used in conjunction with an ultrasonic manipulation system to investigate the possibility of an automated system. The acoustic radiation force is the force that acts on a particle suspended in a fluid when the fluid is excited to vibration. Recent work has investigated the use of such forces to manipulate particles and cells within micromachined fluidic systems [12], [13]. A system has been developed here that allows positioning of particles into lines within a static fluid in a chamber that is open at the end, allowing access for the gripper. Manipulation experiments using these combined methods for particles and biological cells are shown.

## II. DESIGN OF THE MICROGRIPPER

The microgripper has been designed to accomplish three requirements:

- handle objects of a size ranging from 5 to 200  $\mu\text{m}$ ;
- provide real-time force feedback of the gripping force during manipulation;
- demonstrate the capability of being used in aqueous environments in order to handle biological cells.

Fig. 1 shows a solid model of the microgripper. The structures are etched from a silicon-on-insulator (SOI) wafer.

### A. Functional Principle

To pick up an object, the left arm is pushed to the right by the actuator until the gripper arms are closed. This generates a gripping force that deflects the right arm. This deflection is measured by the comb drive for force sensing on the right, as illustrated in Fig. 2. The deflection of the right arm is proportional to the gripping force and is independent of the size or the mechanical properties of the object which is gripped. This would not be the case when using the same comb drive for both actuation and sensing.

### B. Design of the Actuator

Lateral comb drives have been chosen to actuate the gripper. The comb finger electrodes are considered as parallel plates. The driving force  $f_e$  for a single finger pair is given by

$$f_e = \frac{1}{2} \epsilon \frac{tV^2}{d}$$

where  $\epsilon = 8.85 \times 10^{-12} \text{ C}^2/(\text{Nm}^2)$  is the permittivity of air,  $V$  the driving voltage,  $d$  the distance between the plates, and  $t$

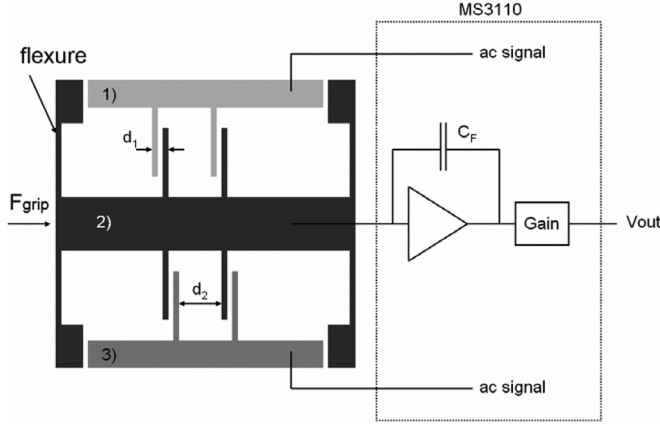


Fig. 3. Capacitive sensor schematic with readout circuitry.

the thickness given by the device layer of the SOI wafer. For a set of  $n$  capacitors, the total driving force  $F_e$  is given by

$$F_e = n\varepsilon \frac{tV^2}{d}.$$

The restoring force  $F_r$  is created by flexure1 to flexure4 shown in Fig. 1.

$$F_r = kx \text{ with } k = 4 \frac{Et w^3}{l^3}$$

where  $x$  is the deflection and  $k$  the spring constant of the system,  $E$  is the Young's modulus of silicon,  $t$  is the wafer thickness,  $w$  is the width of the flexure, and  $l$  is the length of the flexure. Flexure 5 and flexure 6 convert the translational movement of the comb drive into a rotational movement of the gripper arm. The minor bending of these flexures increases the restoring force as well, but their contribution is small and can be neglected. The motion of the end-effector is amplified by a factor of four by transforming the motion of the comb drives in a rotational movement.

### C. Design of the Force Feedback Sensor

As shown in Fig. 3, the right arm transmits the gripping force to the movable capacitor plates of the transverse comb drive. The restoring force  $F_r$  of the sensor is given by

$$F_r = 4 \frac{Et w^3}{l^3} x$$

where  $l$  is the length of the flexures of the sensor and  $x$  the deflection. Again, the bending of the two flexures which convert the rotational motion of the gripper into a translational motion is small and can be neglected. A balanced pair configuration of comb drive plates is used as shown in Fig. 3. Stationary capacitor plates are represented by 1) and 3), while 2) are movable plates.

A signal  $V_{out}$  is generated by the capacitive readout chip MS3110 by MicroSensors [11]. For a gap distance  $d_1 \ll d_2$ ,

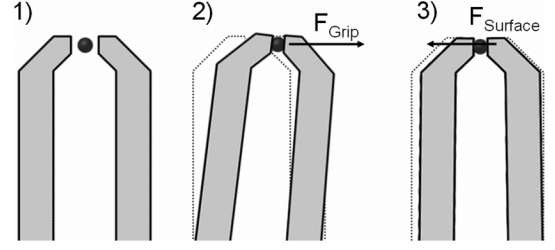


Fig. 4. Forces acting on the right gripper arm used for force sensing during micromanipulation.

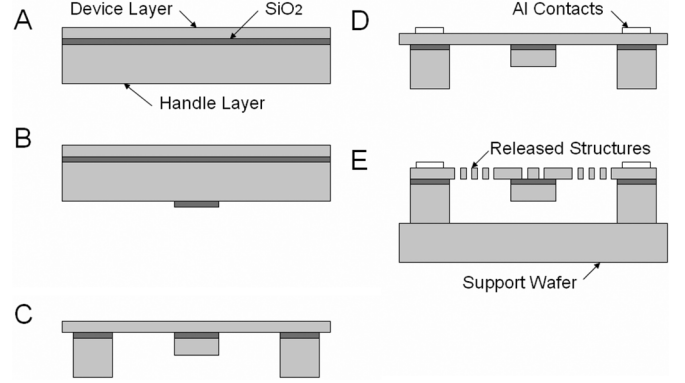


Fig. 5. Fabrication sequence.

the readout chip generates an analog voltage signal  $V_{out}$  proportional to the deflection  $x$

$$V_{out} \propto \text{Gain} \frac{C_1 - C_2}{C_F} \text{ with } C_1 = \varepsilon \frac{Q}{d_1 - x} + \varepsilon \frac{A}{d_2 + x}$$

$$C_2 = \varepsilon \frac{A}{d_1 + x} + \varepsilon \frac{A}{d_2 - x}$$

where  $A$  is the area of the plates and  $\text{Gain}$  and  $C_F$  are programmable on the application-specific integrated circuit.

The range, sensitivity, and resolution of the sensing system are easily varied by changing the length of the flexures. The stiffness of the sensing system is much higher than the stiffness of the actuator. The maximum deflection of the fingertips on the sensor side is  $4 \mu\text{m}$ , corresponding to a  $1 \mu\text{m}$  deflection at the capacitor plates.

An important feature of the force sensor is that it can also be used to measure adhesive forces between the gripper fingers. Fig. 4 shows the forces acting on the right gripper arm during a pick-and-place manipulation. In 1), no forces are acting on the arm. In 2), a positive gripping force  $F_{Grip}$  can be measured, which is caused by the actuator. When the finger tips are close to the object or touching it, as shown in 3), the right arm is pulled to the left by surface forces  $F_{Surface}$ , which is measured as a negative force.

### D. Design of the Gripper Arms

In order to handle biological cells in aqueous environments, the gripper arms must be electrically insulated. To make both mechanical connection and electrical insulation possible, the comb drives are connected to the gripper arm using the handle

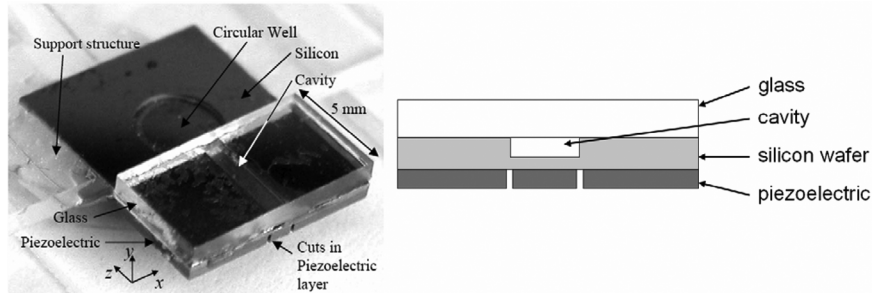


Fig. 6. Photograph and cross-section of the ultrasonic manipulator design.

layer of the SOI wafer as shown in the inset of Fig. 1. The buried oxide and the air gap etched into the device layer insulate the gripper arms from the actuation voltage.

There is a metal contact for wire-bonding for each gripper arm. The electrical potential can be set to a well-defined voltage to eliminate electrostatic effects that may complicate micromanipulation.

Experiments show that the whole length of the gripper arms can be immersed in water. This is sufficient for handling cells. Immersing the comb drives into the water, however, is not possible, since the active part including the actuation comb drives as well as the force sensing comb drives must remain outside the liquid. Three different designs of gripper finger tips have been fabricated with a maximum opening of 50, 100, and 200  $\mu\text{m}$ . The 50 and 100  $\mu\text{m}$  designs can be fully closed. The 200  $\mu\text{m}$  design is used for handling large objects with sizes ranging from 100 to 200  $\mu\text{m}$ .

### III. FABRICATION SEQUENCE

The fabrication sequence is illustrated in Fig. 5 based on the fabrication process presented in [9] and [10].

- A) A silicon-on-insulator wafer with a device layer of 50  $\mu\text{m}$ , a handle layer of 400  $\mu\text{m}$ , and a buried  $\text{SiO}_2$  layer of 2  $\mu\text{m}$  is used for the process.
- B) A 1.5  $\mu\text{m}$  layer of  $\text{SiO}_2$  is deposited on the wafer backside and patterned using reactive ion etching (RIE).
- C) The backside silicon is etched using deep reactive ion etching (DRIE). After etching 200  $\mu\text{m}$ , the  $\text{SiO}_2$  patterned in step B) is removed. Then the remaining 200  $\mu\text{m}$  of silicon is etched. The buried  $\text{SiO}_2$  acts as an etch stop. This procedure creates the step of the thickness of the handle layer. The buried  $\text{SiO}_2$  is etched using RIE.
- D) A 150-nm-thick layer of aluminum is evaporated and patterned by etching the metal. Subsequently, the metal is annealed at a temperature of 450  $^\circ\text{C}$  for 20 min.
- E) The SOI wafer is glued to a silicon support wafer using heat conductive paste. The device layer, including the flexures, comb drives, and gripper arms, is etched using DRIE dry etching. By etching a border around the device, it is released onto the support wafer below the SOI wafer. The dice-free release process protects fragile structures from damage.

The minimum feature size of the structures on device layer is 5  $\mu\text{m}$ , which corresponds to an aspect ratio of 1:10.

### IV. ULTRASONIC MANIPULATOR DESIGN

When a fluid containing a suspension of particles is exposed to ultrasonic vibration, then a force field acts on those particles. These forces arise from the second-order terms in the pressure field, which, when time averaged over the period of the excitation are nonzero, is termed the acoustic radiation force. Recently, micromachined systems have been developed that are capable of positioning particles in distinct and observable lines [12] and [13]. Here an ultrasonic device has been designed to preposition objects prior to mechanical handling. This requires that the fluid is not flowing and that one end of the channel is open in order to allow access to the microgripper. The resultant device is based on the work presented in [12]. The device has useful resonant frequencies at 0.78 and 2.08 MHz in which one and three lines are formed, respectively. The higher frequency has the advantage of the lines' being more tightly aligned due to a higher resulting force field. Consequently, the device is first operated at the lower frequency to approximately position the particles in the center of the chamber and then subsequently at the higher frequency in order to improve alignment. This results in a single precisely aligned line of particles, hence combining the advantages of both frequencies. At one end the channel is open, allowing access for the microgripper. At the other end there is a circular well for introducing the particle suspension using a pipette. Capillary forces cause the fluid to fill the channel. The device is constructed as depicted in Fig. 6. The dimensions of the device are 8.6 mm ( $x$ )  $\times$  1.8 mm ( $y$ )  $\times$  12 mm ( $z$ ). It consists of three layers:

- 1) an upper 1000- $\mu\text{m}$ -thick glass wafer;
- 2) a middle 300- $\mu\text{m}$ -thick silicon wafer with a 200- $\mu\text{m}$ -deep cavity etched into it;
- 3) a lower 500- $\mu\text{m}$ -thick piezoelectric plate.

Cuts in the piezoelectric layer can be seen in Fig. 6. These are used to aid energy concentration inside the fluid chamber. There is an additional cut that cannot be seen to a depth of 40  $\mu\text{m}$  running along the center of the lower electrode of the central piezoelectric element. The pressure fields required to position particles in one or three lines are asymmetric, thus an asymmetric excitation is required. By cutting the electrode of the central piezoelectric element this is possible, as the ac signal (20 V amplitude) is applied to just one of the resulting strips. All other electrodes are grounded.

### V. CHARACTERIZATION

To operate the gripper, it is first glued and wire-bonded directly to a printed circuit board (PCB) with the readout elec-

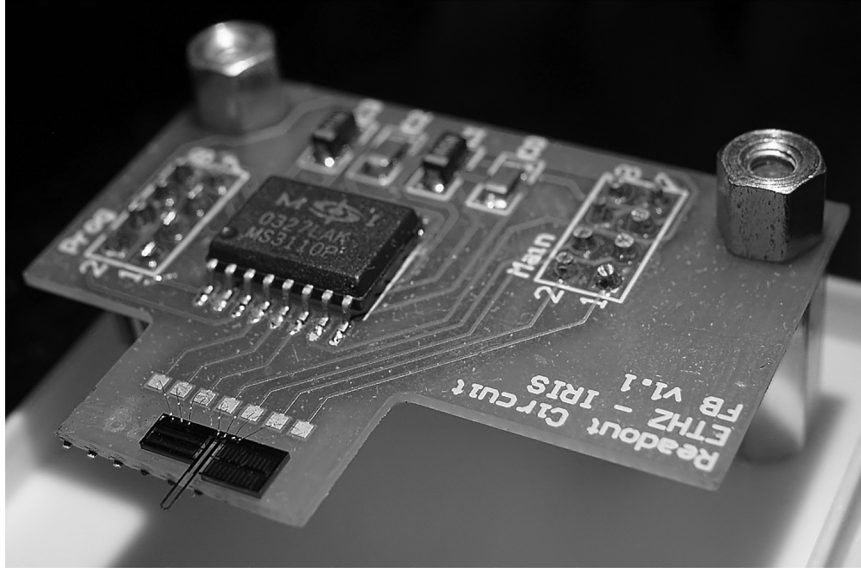


Fig. 7. Gripper glued to the PCB of the readout electronics.

TABLE I  
ACTUATOR DESIGN AND PERFORMANCE

	50 $\mu\text{m}$ opening	100 $\mu\text{m}$ opening	200 $\mu\text{m}$ opening
actuation voltage	0-110V	0-150V	0-150V
gripper opening range	0-50 $\mu\text{m}$	0-100 $\mu\text{m}$	100 $\mu\text{m}$ -200 $\mu\text{m}$
flexure dimensions	900 $\mu\text{m}$ x 10 $\mu\text{m}$ x 50 $\mu\text{m}$		
electrode dimensions	100 $\mu\text{m}$ x 5 $\mu\text{m}$ x 50 $\mu\text{m}$		
gap spacing between electrodes	5 $\mu\text{m}$		

tronics as shown in Fig. 7. Voltages ranging from 0 to 150 V are used for actuation. This creates a deflection of 25  $\mu\text{m}$  in the comb drives. The deflection is amplified by a factor of four resulting in a deflection of 100  $\mu\text{m}$  at the arm tip. Table I summarizes the specifications of the actuator for different opening sizes of the gripper arms.

For calibrating the force sensor, an ACCULAB VI-1 mg microscale was used. The output voltage of the capacitive readout chip was measured by converting the analog output voltage to a digital signal using a 14 bit analog-to-digital converter (men M35). Two different flexure lengths for the force sensor have been used, leading to different ranges and resolutions. The calibration curve shows good linearity. The voltage signal has been filtered with a Boltzmann filter at 20 Hz. Table II summarizes the performance of the sensor for two different designs featuring different flexure lengths.

By increasing the flexure length or decreasing the flexure width, the resolution of the sensor can be further increased. By doing so, it was found that the devices become extremely fragile and handling becomes more difficult. Table III compares the specifications of different microgrippers with integrated force feedback as well as electrostatic microgrippers without integrated force feedback.

It can be seen that the resolution and the sensitivity of gripper presented in this paper is in the same range as for the piezoresistive designs. However, these devices are much larger and are assembled from different parts, making the fabrication of the grippers complicated and expensive. The resolution of an optical atomic force microscope design as presented in [7] is, of course, much higher but requires a complicated setup including a laser light source and photodiodes. Optical force measurements are difficult to perform in liquid due to refraction and distortions of the light beam. The monolithically fabricated devices presented in [8] have a sensitivity that is worse by more than three orders of magnitude, and the actuation range is 50 times smaller. However, comparing performance is difficult, since the devices in [8] are smaller in size as well. The grippers in [3] and [14] do not provide force feedback. The range of the device presented in this paper is five times higher, making it possible to manipulate a wider range of objects.

The device presented in this paper is unique not only due to its high resolution and sensitivity but also because it is monolithically fabricated. More than 100 devices can be fabricated from a single 100 mm wafer. Combined with the low-cost MS3110 readout chip, the gripping system provides an inexpensive alternative to the assembled designs presented in [4]–[7].

TABLE II  
SENSOR DESIGN AND PERFORMANCE

	150 $\mu\text{m}$ flexure	300 $\mu\text{m}$ flexure
linear range	$\pm 2800\mu\text{N}$	$\pm 360\mu\text{N}$
sensitivity*	0.55mV/ $\mu\text{N}$	4.41mV/ $\mu\text{N}$
resolution	520nN	70nN
gap spacing between electrodes $d_1, d_2$	5 $\mu\text{m}, 20\mu\text{m}$	
flexure width, flexure thickness	10 $\mu\text{m}, 50\mu\text{m}$	
electrode dimensions	420 $\mu\text{m}$ x 5 $\mu\text{m}$ x 50 $\mu\text{m}$	
total capacity	4.05pF	
range of capacity	2.1pF – 6.1pF	

\* The sensitivity can be programmed on the ASIC. The values shown here are typical numbers that have been used during the experiments.

TABLE III  
COMPARISON OF DIFFERENT GRIPPER DESIGNS

fabrication	Force sensing	Sensitivity [mV/ $\mu\text{N}$ ]	Resolution [nN]	Actuation	Actuation range [ $\mu\text{m}$ ]	Arm length [mm]	Reference
assembled	piezoresistive		100	piezoelectric	213		[4]
assembled	piezoresistive	1.5		piezoelectric			[5]
assembled	piezoelectric	0.0253	19000	magnetic	300		[6]
assembled	optical (AFM)		0.016	piezoelectric	50		[7]
monolithic	piezoresistive	0.0001		thermal	2	0.1	[8]
monolithic	none	-	-	electrostatic	20	1.0	[3]
monolithic	none	-	-	electrostatic	20	0.5	[14]
monolithic	capacitive	0.55-4.41	70-520	electrostatic	100	3.3	This work

## VI. EXPERIMENTAL RESULTS

Pick-and-place manipulation done in air has been successfully accomplished with glass spheres of sizes ranging from 20 to 90  $\mu\text{m}$ .

Gripping forces of 380  $\mu\text{N}$  have been measured at a driving voltage of 140 V using the design with a maximum gripper opening of 100  $\mu\text{m}$  and a sensor spring length of 150  $\mu\text{m}$ . Fig. 8 shows the gripping force curve during picking and releasing of a 35  $\mu\text{m}$  glass sphere. By slowly opening and closing the gripper arms, negative gripping forces normally ranging from  $-5$  to  $-12$   $\mu\text{N}$  have been measured before and after the gripper is fully closed. These relatively large forces are caused by surface tension forces existing in high humidity environments [7], [15]. The surface tension force  $F_{\text{tens}}$  is given by

$$F_{\text{tens}} = \pi d \gamma$$

where  $d$  is the sphere diameter and  $\gamma$  the liquid surface tension (0.073 N/m for water) [15]. For a 35  $\mu\text{m}$  glass sphere, the surface tension force is calculated as 8.0  $\mu\text{N}$ , which corresponds to experimental results.

Electrostatic forces as well as Van der Waals forces add to the total gripping force as well, but analytical models in [7] and [15] show that these forces are smaller by at least one order of magnitude due to the high roughness of the gripper arms which arise from the dry etching process. The experiment was performed at room temperature with a relative humidity of 52%.

In a second experiment, the ultrasonic device was used to preposition copolymer spheres (Duke Scientific) with a diameter of 74  $\mu\text{m}$ . These particles were suspended in deionized water. A small droplet of solution was placed in the well at the end of the micromachined channel. The spheres have been viewed using a microscope from the top through the glass layer of the ultrasonic device. Fig. 9 illustrates the sequence of the experiment.

- Spheres are suspended in water inside the channel.
- Particles are aligned using the ultrasonic force field. After aligning the spheres the field is switched off. This is necessary, since the gripper arms would disturb the ultrasonic field and cause the spheres not to align correctly.
- The microgripper is moved inside the channel filled with water. A single sphere is gripped.

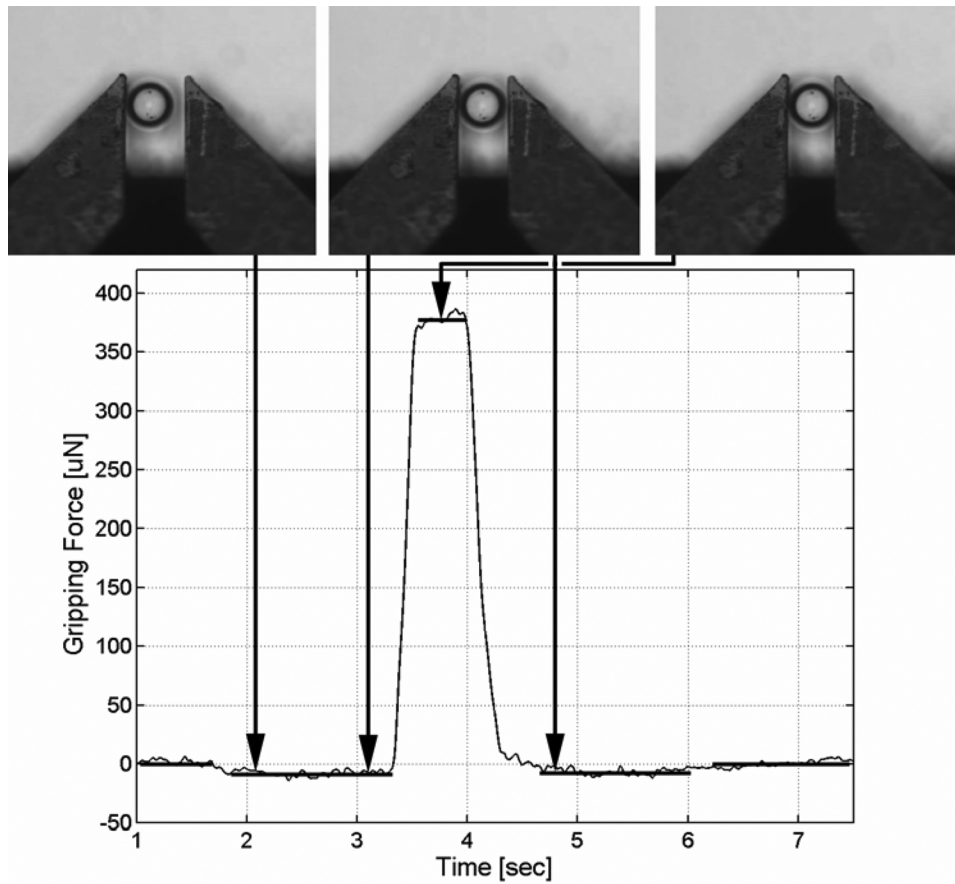


Fig. 8. Measured force during pick-and-place manipulation.

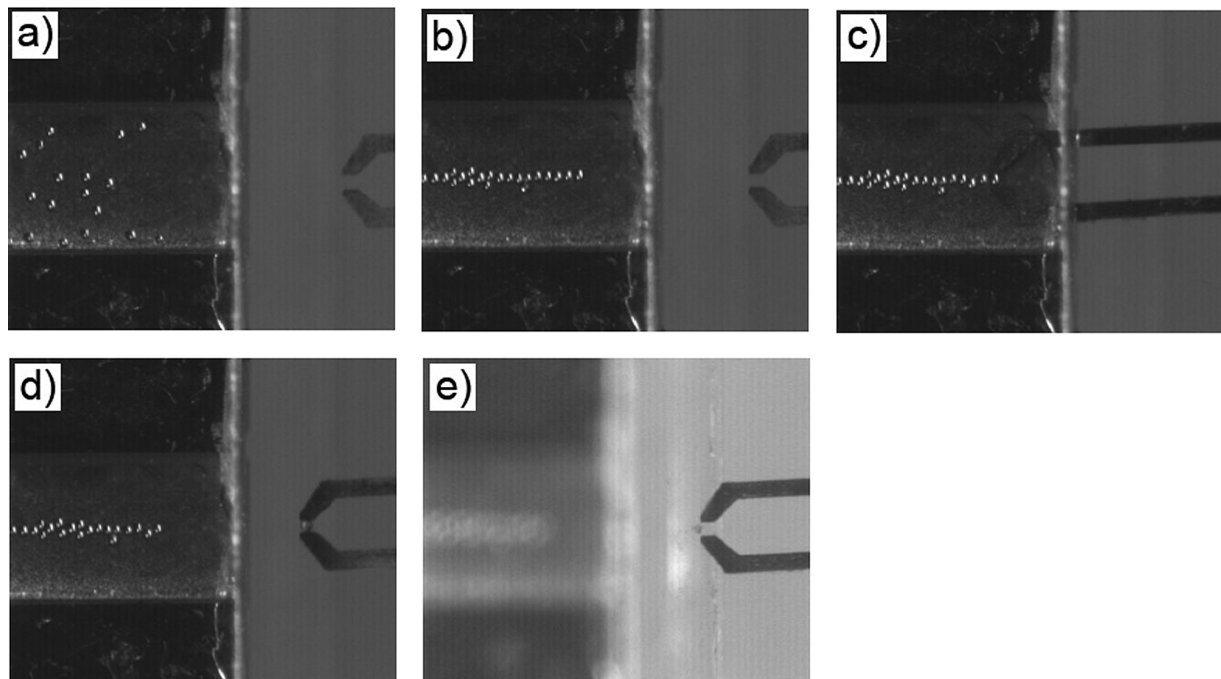


Fig. 9. Spheres are gripped inside the fluid channel of the ultrasonic manipulator.

- d) The gripper is moved back and the sphere is brought outside the channel.
- e) The sphere is released on a glass plate next to the ultrasonic device. The sphere and the gripper arms are covered with water. Releasing the wet sphere onto the dry glass

surface was found to be very reliable. The water dries quickly after depositing the sphere. The ultrasonic field moves the particles to a known and clearly defined position, and thus the speed of the manipulation process can be increased. There is no need to optically search for par-

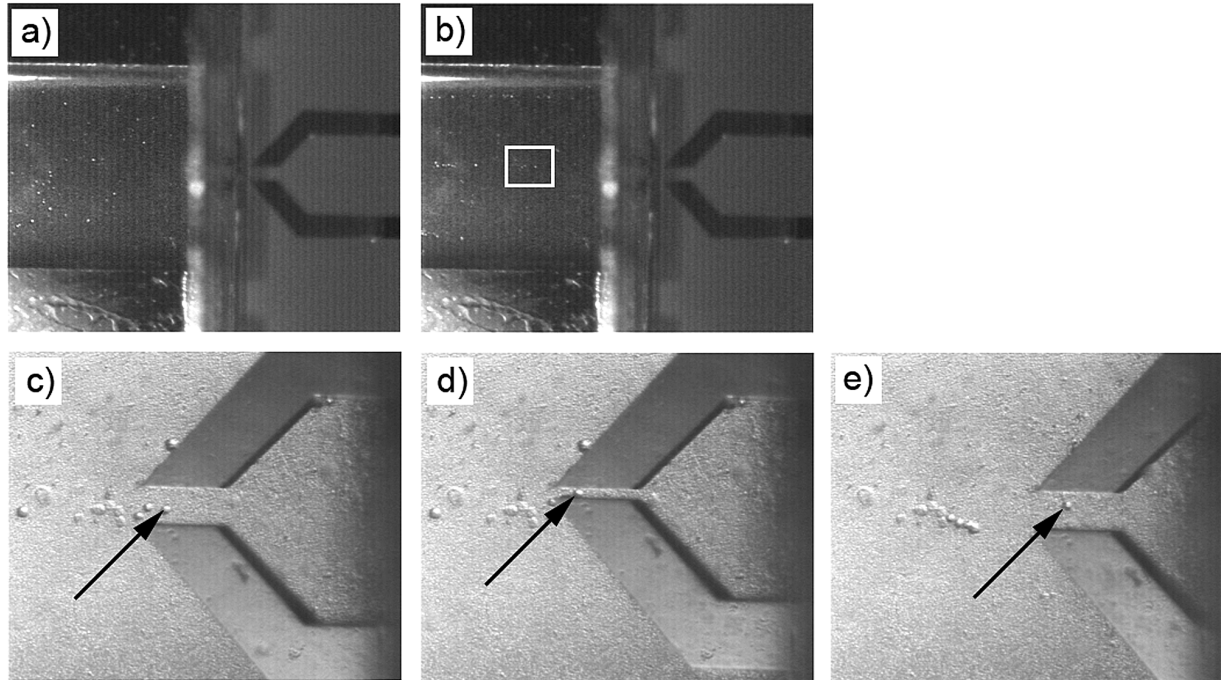


Fig. 10. HeLa cells are gripped and released inside the fluid channel of the ultrasonic manipulator.

ticles in a large area, which is important if a small number of particles is suspended in the fluid only. Additionally, particles close to the channel wall are brought to a location where they can be reached.

The same concept was also demonstrated with biological cells. Suspended HeLa cancer cells with a diameter of approximately  $20\ \mu\text{m}$  have been used. Although manipulating cells is more difficult than manipulating glass spheres due to their smaller size, single cells have been successfully gripped and released inside the fluid channel. The ultrasonic field is normally switched off during manipulation. Sometimes a cell sticks to one of the gripper arms after opening the gripper. It was found that the ultrasonic field can be used to release the cell. Switching the ultrasonic field on creates force-field gradients that pull the cell away from the gripper arms. Fig. 10 shows the sequence of the experiment.

- a) HeLa cells are suspended in liquid.
- b) The cells are aligned in three lines inside the channel. The middle line can be used for picking up the cells with the gripper. Due to the transparency of the HeLa cells, this line are hard to see and thus a higher magnification is used in the following steps.
- c) A smaller field of view is used at the position at the end of the line highlighted by the white rectangle in b). The gripper is inserted into the fluid channel.
- d) A single cell is picked up.
- e) The cell is released at a different position using the ultrasonic force field.

In this experiment, the cell is released inside the same fluid channel. However, cells could also be released in a different container or another fluid channel. Experiments show that there is enough water sticking to the cell and the gripper arms for the cells to survive this treatment. By changing the geometry of the fluid channel and the frequency of the ultrasonic excitation, multiple lines of cells can be formed. The microgripper can be

used as a tool to sort cells by size or mechanical properties. A defined number of cells can be moved to a specific line in the channel or to another container for further use.

## VII. CONCLUSION

A novel design for an electrostatic microgripper with an integrated capacitive force sensor is presented. The gripper fingers open up to  $100\ \mu\text{m}$ , making it possible to manipulate a wide range of objects. The gripper provides real time force feedback with a high sensitivity and is monolithically fabricated. Unlike other sensing methods that provide high-resolution force feedback such as optical methods, the gripper does not require a large or complicated setup. Glass spheres have been successfully manipulated, and the gripping forces as well as the adhesive forces have been measured in real time. A design for an ultrasonic manipulator is presented that is used to align microobjects prior to picking them up with the gripper. The concept has been successfully demonstrated with HeLa cells.

## REFERENCES

- [1] C.-J. Kim, "Silicon electromechanical microgrippers," Ph.D. dissertation, Dept. Mech. Eng., Univ. of California, Berkeley, CA, 1991.
- [2] C.-J. Kim, A. P. Pisano, and R. S. Muller, "Silicon-processed overhanging microgripper," *J. Microelectromech. Syst.*, vol. 1, 1992.
- [3] B. E. Voland, H. Heerlein, and I. W. Rangelow, "Electrostatically driven microgripper," *Microelectron. Eng.*, vol. 61–62, pp. 1015–1023, 2002.
- [4] F. Arai, D. Andou, Y. Nonoda, T. Fukuda, H. Iwata, and K. Itoigawa, "Integrated microendeffector for micromanipulation," *IEEE/ASME Trans. Mechatronics*, vol. 3, no. 1, pp. 17–23, 1998.
- [5] J. Park and W. Moon, "A hybrid-type micro-gripper with an integrated force sensor," *Microsystem Technol. Micro. Nanosyst. Inf. Storage Process. Syst.*, vol. 9, no. 8, pp. 511–519, 2003.
- [6] D. H. Kim, M. G. Lee, B. Kim, and Y. Sun, "A superelastic alloy microgripper with embedded electromagnetic actuators and piezoelectric force sensors: A numerical and experimental study," *Smart Mater. Struct.*, vol. 15, pp. 1265–1272, 2005.
- [7] Y. Zhou and B. J. Nelson, "Adhesion force modeling and measurement for micromanipulation," in *Proc. SPIE Int. Symp. Intell. Syst. Adv. Manufact.*, 1998, vol. V3519, pp. 169–180.



- [8] K. Molhave and O. Hansen, "Electro-thermally actuated microgrippers with integrated force-feedback," *J. Micromech. Microeng.*, vol. 15, no. 6, pp. 1265–1270, 2005.
- [9] Y. Sun, B. J. Nelson, D. P. Potasek, and E. Enikov, "A bulk microfabricated multi-axis capacitive cellular force sensor using transverse comb drives," *J. Micromech. Microeng.*, vol. 12, no. 6, pp. 832–840, 2002.
- [10] Y. Sun, S. N. Fry, D. P. Potasek, D. J. Bell, and B. J. Nelson, "Characterizing fruit fly flight behavior using a microforce sensor with a new comb drive configuration," *J. Microelectromech. Syst.*, vol. 14, pp. 4–11, 2005.
- [11] "Universal capacitive readout IC (MS3110) manual," Irvine Sensors Corp., 2004.
- [12] A. Neild, S. Oberti, A. Haake, and J. Dual, "Finite element modeling of a micro-particle manipulator," *Ultrasonics*, submitted for publication.
- [13] G. M. Dougherty and A. P. Pisano, "Ultrasonic particle manipulation in microchannels using phased co-planar transducers," in *Proc. 12th Int. Conf. Solid State Sens., Actuators Microsyst.*, Boston, MA, 2003, vol. 670, p. 373.
- [14] C. J. Kim, A. P. Pisano, R. S. Muller, and M. G. Lim, "Polysilicon Microtweezers," *Sens. Actuators A Phys.*, vol. 33, pp. 221–227, 1992.
- [15] F. Arai, D. Ando, T. Fukuda, Y. Nonoda, and T. Oota, "Micro manipulation based on micro physics—strategy based on attractive force reduction and stress measurement," in *Proc. 1995 IEEE/RSJ Int. Conf. Intell. Robots Syst. (IROS'95)*, 1995, vol. 2, pp. 263–241.



**Felix Beyeler** (S'06) received the M.Eng. degree in mechanical engineering from the Swiss Federal Institute of Technology, Zurich, in 2004, where he is currently pursuing the Ph.D. degree at the Institute of Robotics and Intelligent Systems.

During his studies he focused on robotics and biomedical engineering. Currently, he is working on the development of novel MEMS devices for micromanipulation and biological research.



**Adrian Neild** received the Ph.D. degree in engineering from the University of Warwick, U.K., in 2003.

He has since become a Postdoctoral Researcher at the Institute for Mechanical Systems, Swiss Federal Institute of Technology, Zurich. His research interests lie in the fields of noncontact ultrasound, micro-machined transducers, and nondestructive evaluation and the use of acoustic radiation force to manipulate small particles in microfluidic systems.



**Stefano Oberti** received the M.Eng. degree in mechanical engineering from the Swiss Federal Institute of Technology, Zurich, in 2004, where he is currently pursuing the Ph.D. degree.

His focus was on micro and nanofabrication and control systems. During his diploma project, he worked on the development of a microsqueeze force sensor useful as contact-free profilometer and viscometer at the IBM Research Laboratory, Rüschlikon, Switzerland. His main research area is ultrasonic manipulation within microfluidic devices.



**Dominik J. Bell** received the M.Eng. degree in aerospace engineering from the University of Bristol, U.K., in 2002 and the M.Phil. degree from the Engineering Department, University of Cambridge, U.K., in 2003. He is currently pursuing the Ph.D. degree at the Institute of Robotics and Intelligent Systems, Swiss Federal Institute of Technology, Zurich.

His research focus is on micro- and nanoelectromechanical systems devices and on wireless sensing and actuation.



**Yu Sun** (S'01–M'03) received the B.S. degree in electrical engineering from Dalian University of Technology, China, in 1996, the M.S. degree from the Institute of Automation, Chinese Academy of Sciences, Beijing, China, in 1999, the M.S. degree in electrical engineering from the University of Minnesota, Minneapolis, in 2001, and the Ph.D. degree in mechanical engineering from the University of Minnesota in 2003.

He held a Research Scientist position at the Swiss Federal Institute of Technology (ETH-Zurich) before joining the faculty of the University of Toronto, Toronto, ON, Canada, where he is an Assistant Professor in the Mechanical and Industrial Engineering Department and is jointly appointed to the Institute of Biomaterials and Biomedical Engineering and Electrical and Computer Engineering Department. He established and directs the Advanced Micro and Nanosystems Laboratory at the University of Toronto. His research areas are MEMS design, fabrication and testing, microrobotic manipulation of biomaterials, cell mechanics, nanofabrication, and nanorobotic manipulation of nanomaterials.

Dr. Sun is a recipient of the University of Minnesota Dissertation Fellowship and the Ontario Early Researcher Award.



**Jürg Dual** received the M.S. and M.Eng. degrees in mechanical engineering from the University of California, Berkeley.

After one year as Visiting Assistant Professor with Cornell University, Ithaca, NY, he joined the Swiss Federal Institute of Technology (ETH), Zurich, as an Assistant Professor. Since 1998, has been a full Professor of mechanics and experimental dynamics with the Center of Mechanics, Institute of Mechanical Systems, ETH Zurich. His research focuses on wave propagation and vibrations in solids

as well as micro- and nanosystem technology. In particular he is interested in both basic research and applications in the area of sensors (viscometry), nondestructive testing, mechanical characterization of microstructures, and gravitational interaction of vibrating systems.

Prof. Dual is a Fellow of ASME and Honorary Member of the German Association for Materials Research and Testing. He received the Latsis Prize from ETH Zurich in 1989 for his dissertation. He received a Fulbright grant.



**Bradley J. Nelson** (M'90) received the B.S. degree in mechanical engineering from the University of Illinois at Urbana-Champaign in 1984, the M.S. degree in mechanical engineering from the University of Minnesota, Minneapolis, in 1987, and the Ph.D. degree in robotics from the School of Computer Science, Carnegie–Mellon University, Pittsburgh, PA, in 1995.

He is a Professor of robotics and intelligent systems with the Swiss Federal Institute of Technology (ETH), Zurich, where he is Head of the Institute of Robotics and Intelligent Systems. He was an Engineer with Honeywell and Motorola and a U.S. Peace Corps Volunteer in Botswana, Africa. He became an Assistant Professor with the University of Illinois at Chicago in 1995, Associate Professor with the University of Minnesota in 1998, and Professor with ETH in 2002. His most recent scientific contributions have been in the area of micro-robotics, biomicrobotics, and nanorobotics, including efforts in robotic micromanipulation, microassembly, MEMS (sensors and actuators), mechanical manipulation of biological cells and tissue, and nanoelectromechanical systems. He has chaired several international workshops and conferences.

Prof. Nelson received a McKnight Land-Grant Professorship, the Office of Naval Research Young Investigator Award, the National Science Foundation Faculty Early Career Development (CAREER) Award, the McKnight Presidential Fellows Award, and the Bronze Tablet. He became a Robotics and Automation Society Distinguished Lecturer in 2003 and received the Best Conference Paper Award at the IEEE 2004 International Conference on Robotics and Automation. He was named to the 2005 "Scientific American 50," *Scientific American's* annual list recognizing outstanding acts of leadership in science and technology, for his work in nanorobotic manufacturing. He serves on or has been a member of the editorial boards of the IEEE TRANSACTIONS ON ROBOTICS, the *Journal of Micromechanics*, and the IEEE ROBOTICS AND AUTOMATION MAGAZINE, and is a Senior Editor of the IEEE TRANSACTIONS ON NANOTECHNOLOGY.